International Journal of Nanomedicine

Dovepress
open access to scientific and medical research

Open Access Full Text Article

ORIGINAL RESEARCH

A Novel Calcium Phosphate–Based Nanocomposite for Augmentation of Cortical Bone Trajectory Screw Fixation

Yuetian Wang[1,*], Chun Liu[2,*], Huiling Liu[3], Haoyong Fu[1], Chunde Li[1], Lei Yang[3,4], Haolin Sun[1]

[1]Department of Orthopedics, Peking University First Hospital, Beijing, People's Republic of China; [2]Medical Research Centre, Changzhou Second People's Hospital Affiliated to Nanjing Medical University, Jiangsu, People's Republic of China; [3]Institute of Orthopedics, Department of Orthopedics, Soochow University, Suzhou, People's Republic of China; [4]Center for Health Sciences and Engineering (CHSE), School of Health Sciences and Biomedical Engineering, Hebei University of Technology, Tianjin, People's Republic of China

*These authors contributed equally to this work

Correspondence: Lei Yang; Haolin Sun, Tel +86 13681146156, Email ylei@hebut.edu.cn; sunhaolin@vip.163.com

Purpose: To evaluate the effect of cement augmentation of cortical bone trajectory (CBT) screws using a novel calcium phosphate–based nanocomposite (CPN).

Material and Methods: CBT screws were placed into cadaveric lumbar vertebrae. Depending on the material used for augmentation, they were divided into the following three groups: CPN, polymethylmethacrylate (PMMA), and control. Radiological imaging was used to evaluate the cement dispersion. Biomechanical tests were conducted to measure the stability of CBT screws. A rat cranial defect model was used to evaluate biodegradation and osseointegration of the CPN.

Results: After cement augmentation, the CPN tended to disperse into the distal part of the screws, whereas PMMA remained limited to the proximal part of the screws ($P < 0.05$). As for cement morphology, the CPN tended to form a concentrated mass, whereas PMMA arranged itself as a scattered cement cloud, but the difference was not significant ($P > 0.05$). The axial pullout test showed that the average maximal pullout force (Fmax) of CPN-augmented CBT screws was similar to that of the PMMA group (CPN, 1639.56 ± 358.21 N vs PMMA, 1778.45 ± 399.83 N; $P = 0.745$) and was significantly greater than that of the control group (1019.01 ± 371.98 N; $P < 0.05$). The average torque value in the CPN group was higher than that in the control group (CPN, 1.51 ± 0.78 N·m vs control, 0.97 ± 0.58 N·m) and lower than that in the PMMA group (1.93 ± 0.81 N·m), but there were no statistically significant differences ($P > 0.05$). The CPN could be biodegraded and gradually replaced by newly formed bone tissue after 12 weeks in a rat cranial defect model.

Conclusion: The biocompatible CPN could be a valuable augmentation material to enhance CBT screw stability.

Keywords: cement augmentation, CBT screws, osteoporotic spine, PMMA, CPN

Introduction

Posterior pedicle screw fixation systems have widely been used in the treatment of spinal diseases. However, pedicle screw loosening, especially in the spine with lower bone quality, is still a common problem faced by surgeons. It has been reported that the rate of screw loosening in osteoporotic patients could be ≤60%,[1] which increases the risk of instrument failure. The cortical bone trajectory (CBT) screw technique is an existing method used to enhance screw anchorage and it works by increasing the contact area between the screw and the more rigid cortical bone.[2] Due to the cranial screw insertion occurring through a caudomedial starting point, the CBT screw technique achieves less-invasive fixation than traditional pedicle screws by limiting dissection of the superior facet joints and reducing muscle dissection and retraction, which has led to its increasing popularity among spinal surgeons.[3,4] However, some studies have concluded that the stability of CBT screws cannot surpass that of traditional pedicle screws.[5,6] Shorter and smaller screws inserted in vertebrae may incur higher stress, and micro-motions of the screws and bone encroachment around the screws accelerate once screw loosening occurs.[7] It has also been reported that the loosening rate of CBT screws in

Received: 16 March 2022
Accepted: 26 June 2022
Published: 9 July 2022

clinical practice is up to 6.5%.[8] Thus, there is a need to further enhance CBT screw stability, especially given the increasing number of aging patients.

The cement augmentation technique may be a useful method to increase pedicle screw stability. However, early screw loosening remains a concern when treating patients with severe bone loss. While increasing the injected cement volume would strengthen the holding power, it simultaneously would raise the rate of complications related to cement, such as cement leakage or even pulmonary cement embolism.[9,10] Currently, the most widely used augmentation material is polymethylmethacrylate (PMMA), which has some advantages, such as biocompatibility, injectability, and good mechanical properties.[11,12] However, PMMA has a high exothermic polymerization temperature, monomer toxicity, and a high elastic modulus, and has neither the characteristic of good osteoinduction nor biodegradability.[11,13,14] These drawbacks of PMMA have been shown to cause side effects in clinical practice, such as nerve injury, great removal difficulty, and surgical site infection.[15–17] As a potential alternative cement to PMMA, calcium phosphate cement (CPC) has characteristics of self-curing, biocompatibility, osteoconductivity, and resorbability.[18–20] However, some disadvantages in clinical application, such as the imbalance of biodegradation and bone regeneration and the lower initial mechanical strength than PMMA, require modifications of this material.[21–23] Considering the nanostructured nature of bone, nanomaterials have been incorporated into existing cement to improve their mechanical and biological properties for the use in bone augmentation, filling bone defects, and bone tissue regeneration.[12,24,25] These modified materials tend to have better biocompatibility, osteoinduction, and biodegradation than traditional cements. Because the inclusion of nanomaterials can effectively supplement the deficiency of existing cement, a reinforced but injectable nanocomposite consisting of the self-curing bioabsorbable CPC with a nanoscale starch network was designed.[26–28]

In a biomechanical study, we had demonstrated that PMMA augmentation is capable of increasing CBT screw stability,[29] and in previous studies on the augmentation of cannulated pedicle screws, CPN demonstrated biomechanical strength similar to that of PMMA.[27,28] In this study, we tried to apply the CPN for CBT screw augmentation to integrate the advantages of both the novel nanomaterial and the unique trajectory fixation system. We evaluated the biomechanical properties of CPN in comparison with PMMA to explore the prospect of clinical application.

Materials and Methods

The CPN was prepared in accordance with the method provided by previously published studies.[27,28] To confirm the successful preparation of CPN, some of its properties were measured in this study. The setting times were measured following the method stated in the ASTM C266-89 and other well-known studies.[30] The rheological characterization of CPN was achieved using a DHR2 rheometer to reflect the viscosity of the prepared CPN. In addition, the compressive strengths of the CPN and PMMA were tested by uniaxial compression tests to verify the mechanical strength. Then, cadaveric lumbar specimens were processed and CBT screws were placed with the help of designed three-dimensionally (3D) printed templates. After that, the prepared CPN and PMMA were employed to enhance the CBT screw fixation. Next, the radiological evaluation and biomechanical tests were conducted to evaluate the cement dispersion patterns and biomechanical properties. Additionally, a rat cranial defect model was used to observe the CPN biodegradation and osseointegration.

CPN and PMMA Preparation

As previously reported,[27,28] the CPN powder contained 60 wt% CPC powder consisting of 90 wt% α-tricalcium phosphate (Dingan Science and Technology, Suzhou, China) and 10 wt% analytical dicalcium phosphate dihydrate, 20 wt% nano-scale starch [JianjieIndustrial (Group) Co., LTD, Zhengzhou, China], and 20 wt% barium sulfate powder ($BaSO_4$; Sigma Aldrich, St. Louis, MO, USA]. The setting liquid of the CPN was 0.25 mol/L sodium hydrogen phosphate solution (Sigma Aldrich), and the CPN powder was mixed with the setting liquid at 21°C (at the liquid-to-powder ratio of 0.5 mL/g). For the comparison, PMMA (Mendec Spine; Tecres SPA, Sommacampagna, Italy) was also set at 21°C with a powder-to-liquid ratio of 2:1 in accordance with the manufacturer's instructions. The curing times of the CPN and PMMA were recorded.

Setting Times and Rheological Measurements

In line with previous studies,[26,30] the initial and final setting times of the cement samples were tested using a Gilmore indenter end-capped with a light and thick needle and a heavy and thin needle, respectively. Both needles were dropped onto the cement surface, and indentation was repeated every minute until there was no perceptible mark left on the surface. The total times using different needles were defined as the initial and final setting times. Each test was repeated five times.

Rheological characterization of the CPN was achieved using a DHR2 rheometer (TA Instruments, New Castle, DE, USA). The measurement started 2 min after mixing of the solid and liquid phases, and then the samples were added on a diameter of 40-mm cone-plate geometry and stabilized for 5 min in the rheometer. To investigate the viscosity of the CPN, the measurements were plotted over a frequency range of 0.1–10 Hz by applying 1% strain at 25°C by dynamic mechanical analyses.

Compression Tests of CPN and PMMA

To evaluate the basic mechanical properties of the CPN, we tested the compressive strengths of the CPN and PMMA by uniaxial compression tests.[26,27] The cement was set in a cylindrical stainless-steel mold (6 mm in diameter and 12 mm in length), and the cement bars were uniaxially compressed by a mechanical tester (HY-1080; Heng Yi Precision Instrument Co., Shanghai, China) with a 10-kN load cell (gauge precision, 0.5 N) at a crosshead speed of 0.5 mm/min. Stress–strain curve data were collected, and the maximum stress value was taken as the compressive strength. Each type of cement was tested five times.

Cadaveric Specimen Processing

This cadaveric study was approved by the Human Subjects Institutional Review Board of Peking University First Hospital (No. 2021–209) and Changzhou Second People's Hospital (MR-32-21-013367). Lumbar vertebrae (L1–L5) without tumors, fractures, and deformities were harvested from five fresh postmortem human subjects ranging in age from 63 to 81 years. Each specimen was evaluated by dual-energy X-ray absorptiometry to confirm the reduced bone quality. These specimens were stored at −20°C until further procedures were performed.

Design of 3D Templates

After obtaining the fresh lumbar vertebrae, high-resolution computed tomography (CT) imaging was performed to collect data to prepare the 3D-printed templates. The 3D-printed templates were designed to completely fit the posterior bone structure of the lumbar vertebrae. Their navigation channels were based on the cortical bone trajectory; the screw entry point was selected at the isthmus, an intersection point of the mid-vertical line of the superior facet joint, and a horizontal line 1 mm below the ipsilateral transverse process. The screw insertion direction was from caudal to cephalic in the sagittal plane, diverging inward to outward in the horizontal plane to ensure sufficient contact of the inserted screws with the dorsal cortex, the posterior medial and the anterior lateral pedicle walls, and the cambered surface of the vertebral body.

Screw Placements and Cement Augmentation

Forty-nine cement-injectable cannulated CBT screws made of Ti6Al4V with an outer diameter of 5.5 mm and a length of 40 mm (Premier, WGB1Z-7-01; Weigao Orthopaedic Device, Weihai, China) were employed. The specimens were rewarmed at room temperature for 24 hours, and soft tissues were removed to expose the posterior bony area of the specimens for the 3D-printed templates to adhere to. Then, an electric drill with a bit 2.5 mm in diameter was driven into the vertebra through the navigation channel. Next, a guidewire was inserted into the hole, and a cannulated screw tap with a 5.5 mm outer diameter was used for tapping the screw trajectory. Finally, a CBT screw was inserted along the tapping direction by a screwdriver. All of the available screws were placed using the same method by an experienced spinal surgeon (Figure 1).

Following the initial mixture of the augmentation materials (about 6 min for CPN and 4.5 min for PMMA), a toothpaste-like material of 1.0 mL of the CPN was loaded by a customized syringe and then injected into each of the selected screws through the cement push rods. The cement type in each screw is summarized in Table 1.

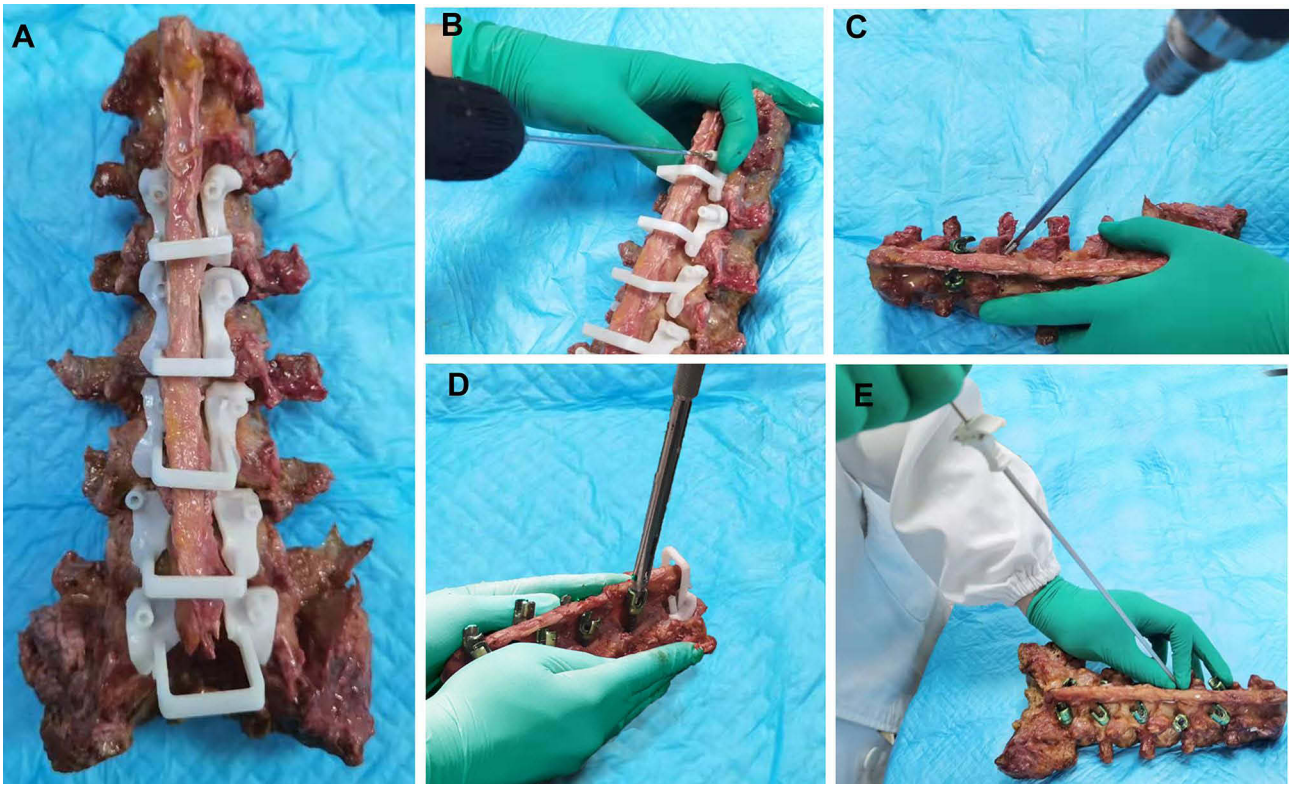

Figure 1 Cortical bone trajectory (CBT) screw placement under the guidance of 3D-printed templates and cement injection.
Notes: (**A**) The templates were positioned correctly in close contact with the posterior bony area after all posterior soft tissue was removed from the cadaveric specimens. (**B**) An electric drill with a bit 2.5 mm in diameter was driven into the vertebra along the direction of the template's channel. (**C**) A Kirschner wire was inserted in the needle lumen, and a cannulated screw tap 4.5 mm in outer diameter was used for tapping according to the guidance of the wire. (**D**) A screw was inserted following the CBT trajectory. (**E**) The cement was injected in the selected screws by a push rod.
Abbreviation: CBT, cortical bone trajectory.

Radiological Evaluation

After screw insertion, plain radiographs and CT images were collected to evaluate the accuracy of the screw placements. The angle deviations in the sagittal and transverse planes between the planned and actual screw positions were measured. After the different augmentation materials were injected, plain radiographs and CT images were collected again to evaluate the cement dispersion. We performed a 3D reconstruction based on the CT data to measure the volume of the dispersed augmentation materials. As the lateral holes region of the screws occupied the first third of the screw length, we chose a demarcation point that bisected the first third of the whole screw; then, the cement cloud was divided into two parts, with the part closer to the screw head defined as the front volume and that closer to the screw tail defined as the rear volume. The specimens were subsequently split into individual vertebral bodies, and the X-ray axial view of each single vertebral body was collected. Each cadaveric lumbar specimen was divided into a pedicle zone and a vertebral body zone on the axial view, and the cement cloud was identified and categorized according to the relevant zones. On the axial view of CT scans, the morphology of the distributed cement was described as a concentrated (C) type, in which the cement was concentrated around the screw in a kind of round mass, or a scattered (S) type, where the injected cement was randomly scattered, spotted, or linearly distributed around the screw with some radiolucent space in the cement.[29] The radiological evaluation of cement-augmented CBT screws was shown in Figure 2.

Biomechanical Tests

Some vertebrae were embedded in cylindric bases of self-curing denture acrylic (Boer Chemical Co., Ltd., Shanghai, China) with a screw positioned along the axis of the cylinder, leaving the screw head exposed. A material testing machine (55 MT Universal Testing Machine; Instron, Norwood, MA, USA) was employed to test the maximum torque values.

Table 1 Information and Characterization of Cadaver Specimens

Cadaver Specimens	Vertebra	Age (Years)	Mean BMD (g/cm^2)	Augmentation Materials Injected on the Left Side	Cement Volume Injected on the Left Side (mL)	Augmentation Materials Injected on the Right Side	Cement Volume Injected on the Right Side (mL)	Biomechanical Test
1	L1	81	0.792	Control	0	—	—	Torsion test
	L2			CPN	1	Control	0	Torsion test
	L3			Control	0	Control	0	Torsion test
	L4			CPN	1	CPN	1	Torsion test
	L5			PMMA	1	PMMA	1	Torsion test
2	L1	63	0.822	Control	0	CPN	1	Torsion test
	L2			PMMA	1	PMMA	1	Torsion test
	L3			PMMA	1	CPN	1	Torsion test
	L4			PMMA	1	Control	0	Torsion test
	L5			PMMA	1	CPN	1	Torsion test
3	L3	78	0.741	PMMA	1	CPN	1	Torsion test
	L4			PMMA	1	Control	0	Torsion test
	L5			CPN	1	Control	0	Torsion test
	L1			Control	0	PMMA	1	Pullout test
	L2			PMMA	1	CPN	1	Pullout test
4	L1	70	0.783	CPN	1	Control	0	Pullout test
	L2			PMMA	1	Control	0	Pullout test
	L3			CPN	1	PMMA	1	Pullout test
	L4			Control	0	CPN	1	Pullout test
	L5			Control	0	PMMA	1	Pullout test
5	L1	67	0.802	PMMA	1	CPN	1	Pullout test
	L2			CPN	1	Control	0	Pullout test
	L3			PMMA	1	Control	0	Pullout test
	L4			CPN	1	PMMA	1	Pullout test
	L5			Control	0	CPN	1	Pullout test

Abbreviations: BMD, bone mineral density; CPN, calcium phosphate–based nanocomposite; PMMA, polymethylmethacrylate.

The screw head was connected to the load frame and rotated counter-clockwise at a rate of 0.5°/s along the screw axis. The torque–angle curve was collected in real time, and testing was performed until the torque value sharply decreased to acquire the maximum torque values (Figure 3A).

The other specimens were sealed in cubic denture base resins to facilitate fixation on a special jig, which could be adjusted to ensure that each screw was pulled along its long axis. After each sample was tightly clamped, each screw was pulled at a constant speed of 5 mm/min until screw loosening; then, the force–displacement curve was recorded. The maximum pullout force (Fmax) was defined as the value at which the load peaked and then sharply decreased with increasing displacement (Figure 3B).

Histological Analysis

A rat cranial defect model was employed to evaluate the biodegradation and osseointegration of the CPN. The animal study was approved by the Animal Care and Use Committee of Soochow University (Approval No. SUDA20200707A03) and followed the Guide for the Care and Use of Laboratory Animals.

The rats (weighing about 200 g) were first anesthetized and placed on a heating pad. After disinfection for three times, the skin was incised at the middle of the skull to remove the underlying periosteum, and a craniotomy defect was created using a 6-mm-diameter electric ring drill without damaging the brain. The rats were divided into two groups: the Blank group, without cement (n=6), and the CPN group (n=6), with the CPN implanted into the defects. Finally, the skull skin was closed by continuous sutures. The rats in both groups were killed at 4 weeks (n = 3) and 12 weeks (n = 3) after

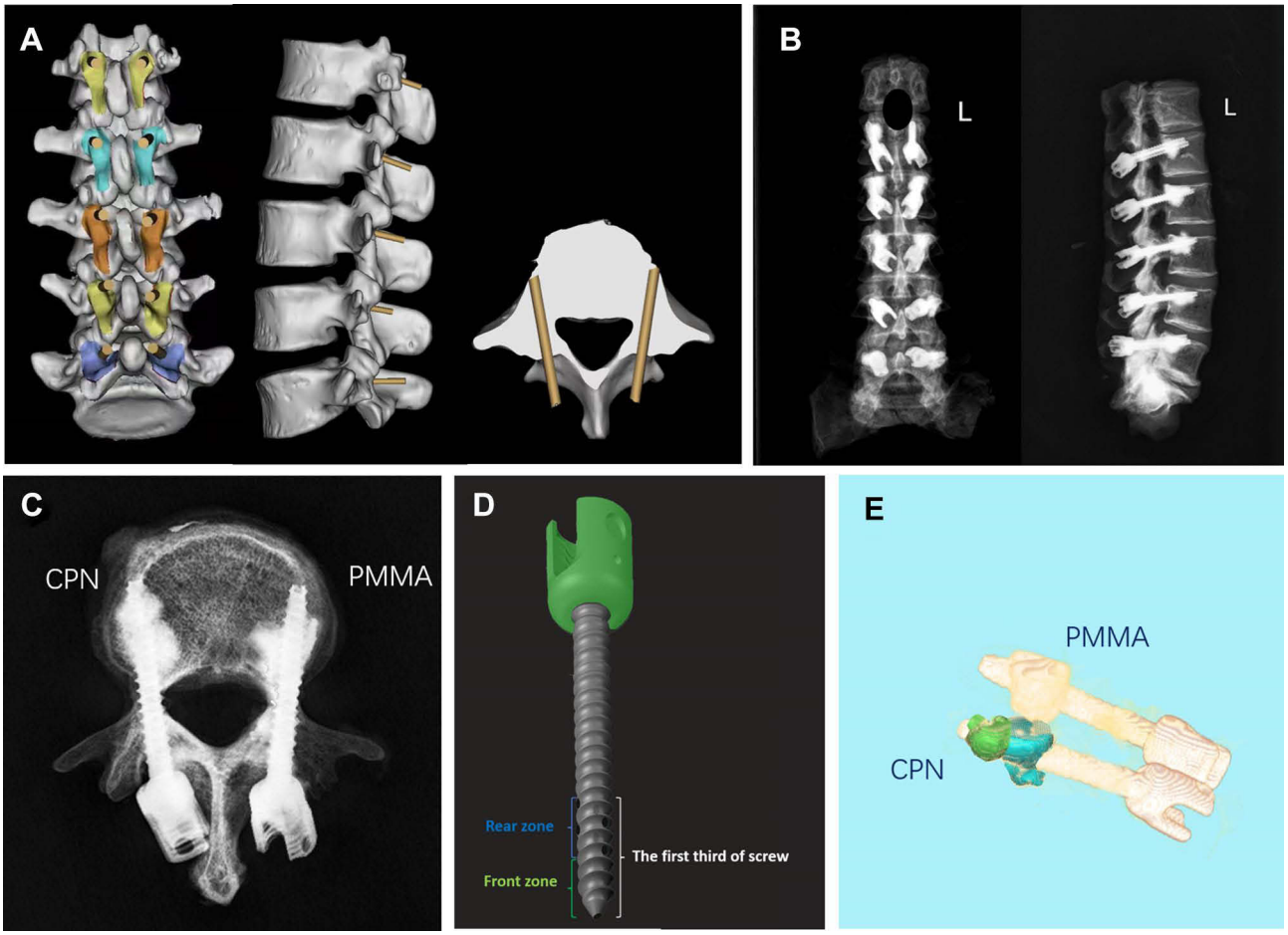

Figure 2 Radiological evaluation of cement-augmented cortical bone trajectory (CBT) screws.
Notes: (**A**) A schematic revealing the design of a 3D-printed template according to the reconstruction from computed tomography data. (**B**) X-ray anteroposterior and lateral views of the specimen after inserting the screws and cement augmentation. (**C**) X-ray axial view of the cement mass. (**D**) The diagram of the CBT screw and the demarcation point that bisects the first third of the whole screw. (**E**) The total volume of bone cement was divided into two parts; the green part is the rear volume and the blue part is the front volume.
Abbreviations: CPN, calcium phosphate–based nanocomposite; PMMA, polymethylmethacrylate.

cement implantation. The skull specimens were collected, fixed with 10% formalin solution for three days, and then decalcified in 10% EDTA solution (Aladdin Chemical Inc., Shanghai, China). After decalcification, the samples were embedded by paraffin, and sliced into 5-μm-thick sections for hematoxylin and eosin (H&E) staining. Next, the slices were observed with a microscope (Olympus, Tokyo, Japan).

Statistical Analysis

Statistical analysis was performed using SPSS version 23.0 (IBM Corporation, Armonk, NY, USA). The data are expressed as mean ± standard deviation values. The chi-square and Fisher's exact probability tests were used for categorical variables. One-way analysis of variance was used to detect differences between the groups. Statistical significance was defined as $P < 0.05$.

Results

Characterization of the CPN

Figure 4A shows the curing process of the cements. The initial setting time of the CPN was 13.54 min and that of PMMA was 14.96 min (P = 0.668), while the final setting time of the CPN was 20.16 min and that of PMMA was 21.76 min (P =

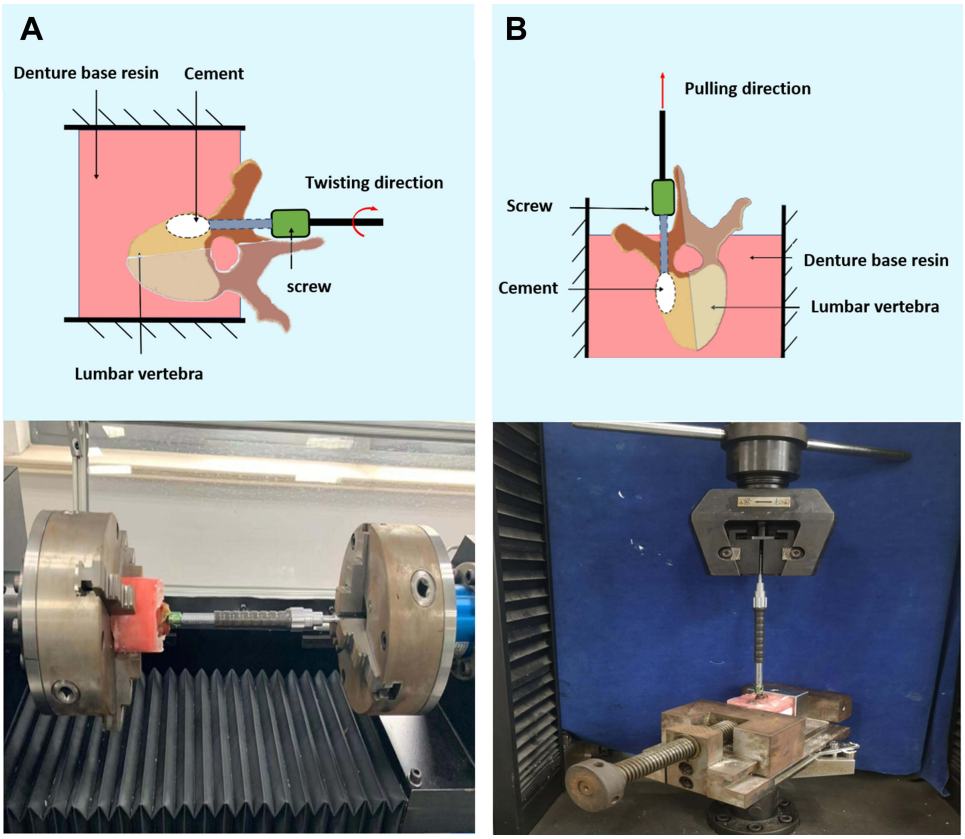

Figure 3 Biomechanical testing of cemented cortical bone trajectory screws.
Notes: (**A**) torsion test and (**B**) axial pullout test.

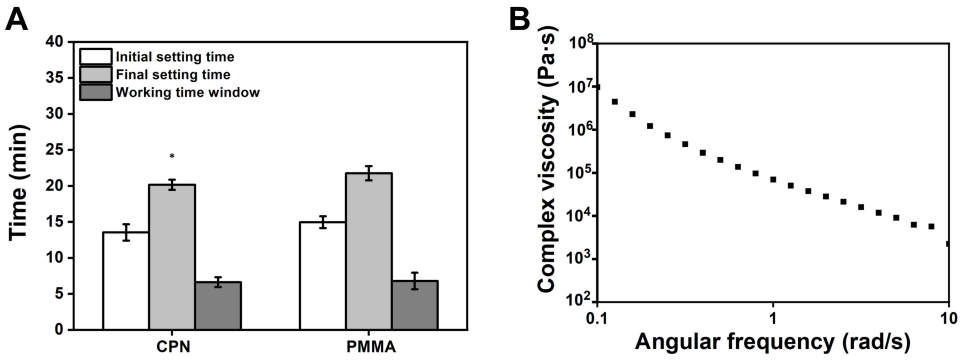

Figure 4 The results of the setting time and rheological properties.
Notes: (**A**) The setting times of CPN and PMMA; CPN: n = 5, PMMA: n = 5 (**B**) The rheological properties of CPN. *P < 0.05 vs the PMMA group.
Abbreviations: CPN, calcium phosphate–based nanocomposite; PMMA, polymethylmethacrylate.

0.019). Additionally, the working time window was 6.62 min for the CPN and 6.8 min for PMMA, but the difference was not statistically significant (P = 0.771).

The frequency-dependent dynamic property of the CPN is shown in Figure 4B. The viscosity of the CPN decreased with the increase of angular frequency from 0.1 to 10 rad/s, and eventually maintained at 10^4 Pa·s.

The uniaxial compression tests showed that the compressive strength of the CPN could reach about half of that of PMMA (40.15 ± 2.93 vs 86.2 ± 4.60 MPa) (Figure 5).

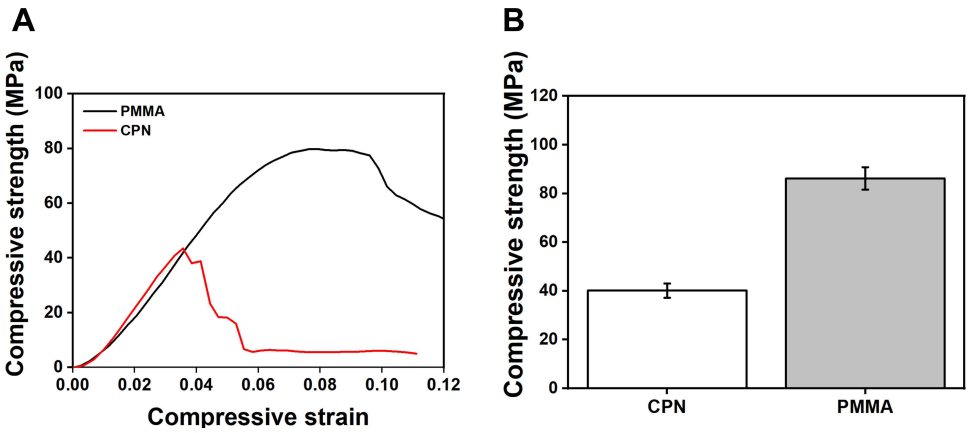

Figure 5 The results of compressive tests.
Notes: (**A**) Typical stress–strain curves of CPN and PMMA and (**B**) average compressive strength of CPN and PMMA.
Abbreviations: CPN, calcium phosphate–based nanocomposite; PMMA, polymethylmethacrylate.

Screw Placements and Cement Augmentation

Forty-nine screws were inserted into the vertebrae following the cortical bone trajectory; of these, 16 were augmented by the CPN, 17 were augmented by PMMA, and 16 were nonaugmented. With the help of the 3D-printed templates, the mean angular deviations in the sagittal and transverse planes were calculated to be 2.26° ± 1.08° and 1.86° ± 0.92°, respectively.

Radiological Evaluation of the Cement Dispersion

The real cement cloud volumes of the CPN and PMMA were 800.31 ± 80.15 mm^3 and 793.12 ± 64.29 mm^3, respectively ($P = 0.777$). The CPN was more inclined to disperse into the vertebral body zone, whereas PMMA was more likely to remain located in the pedicle zone ($P < 0.05$). This result was consistent with the finding of the front volume of the CPN being higher than that of PMMA ($P = 0.006$).

Regarding the cement cloud morphology, there were 26 C-type cement clouds and seven S-type cement clouds. The cement in the CPN group tended to form a concentrated mass (14 C-type clouds vs 2 S-type clouds), whereas the cement in the PMMA group was inclined to shape into a scattered cement cloud (12 C-type clouds vs 5 S-type clouds). However, the difference was not statistically significant ($P > 0.05$).

Biomechanical Properties of CBT Screw Augmentation

Figure 6A and B showed the typical biomechanical curves of the torsion tests and pullout tests with different augmentation materials, respectively. The average torque value in the CPN group was higher than that in the control group (CPN, 1.51 ± 0.78 N·m vs control, 0.97 ± 0.58 N·m) and lower than that in the PMMA group (1.93 ± 0.81 N·m), without any statistically significant differences ($P > 0.05$). The average torque value in the PMMA group was significantly higher than that in the control group ($P = 0.033$) (Figure 6C). The pullout test showed that the average Fmax of cement-augmented CBT in the CPN group was similar to that in the PMMA group (CPN, 1639.56 ± 358.21 N vs PMMA, 1778.45 ± 399.83 N; $P = 0.745$), which was significantly greater than that in the control group (1019.01 ± 371.98 N, $P < 0.05$) (Figure 6D).

Histological Observation

The H&E–stained histological sections (Figure 7) showed that the CPN implant did not collapse after 4 weeks. However, the edge of the CPN sample started biodegradation and the newly formed bone tissue came to occupy the vacancy left by the resorbed CPN clump after 12 weeks. The new bone tissue made a tight contact with the boundary of the residual CPN clump, thereby maintaining a stiff bone–cement interface.

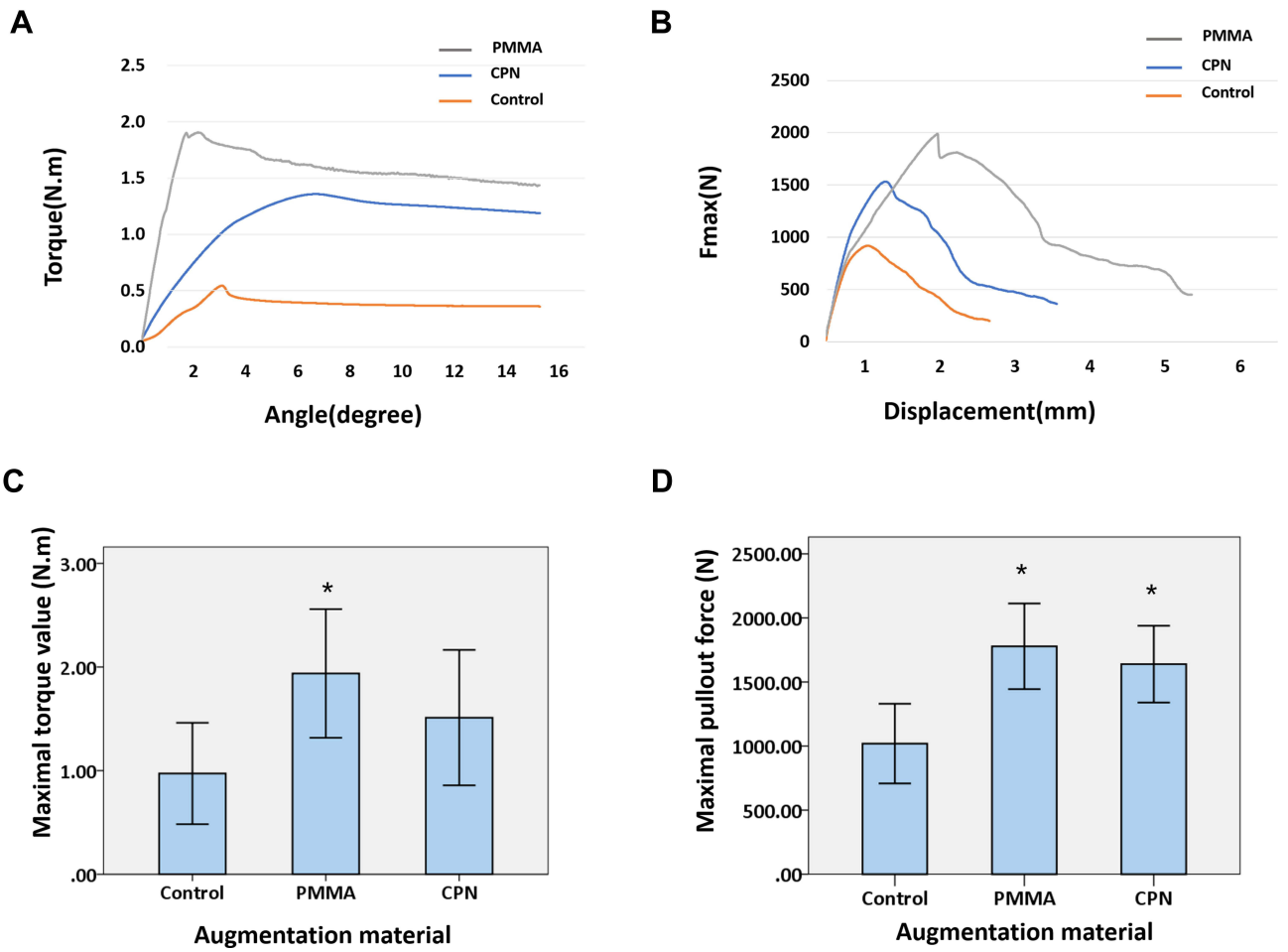

Figure 6 Results of biomechanical tests.
Notes: (**A**) Typical torque–angle curves of the torsion tests with different augmentation materials. (**B**) Typical Fmax–displacement curves of the pullout tests with different augmentation materials. (**C**) Statistical results of the average maximal torque and (**D**) average maximal pullout force of cortical bone trajectory screws augmented by different cements. *P < 0.05 vs the control group.
Abbreviations: CPN, calcium phosphate–based nanocomposite; PMMA, polymethylmethacrylate.

Discussion

CBT screws are designed to increase fixation stability by increasing contact between the screw and the harder cortical bone, which has been confirmed by various biomechanical studies.[35–38] However, some studies have argued that CBT screws do not always outperform traditional pedicle screws in biomechanical tests. For example, in a cadaveric biomechanical study, Wray et al[5] showed that there were no significant differences between CBT screws and traditional pedicle screws in terms of pullout strength and toggle resistance, while Akpolat et al[6] reported that CBT screws showed a fatigue performance inferior to that of traditional pedicle screws. To further enhance the anchorage of CBT screws in the spine with reduced bone stock, we conducted a biomechanical study on PMMA-augmented CBT screws.[29] According to our results, PMMA augmentation is a useful method for increasing CBT screw stability, and the cement injection volume is recommended to be 1 mL for each screw. In the current study, we also showed that the cemented screws had significantly higher biomechanical strength than the nonaugmented screws, which further verified the feasibility and effectiveness of this combined technique.

The cement augmentation technique usually is used to increase the holding power of pedicle screws placed in a traditional trajectory. The augmentation effect could be influenced variably by different kinds of materials. PMMA is the most widely used material, and previous studies have found that it tends to provide the highest biomechanical strength.[17,39,40] However, the aforementioned drawbacks of PMMA leave room for further explorations of the

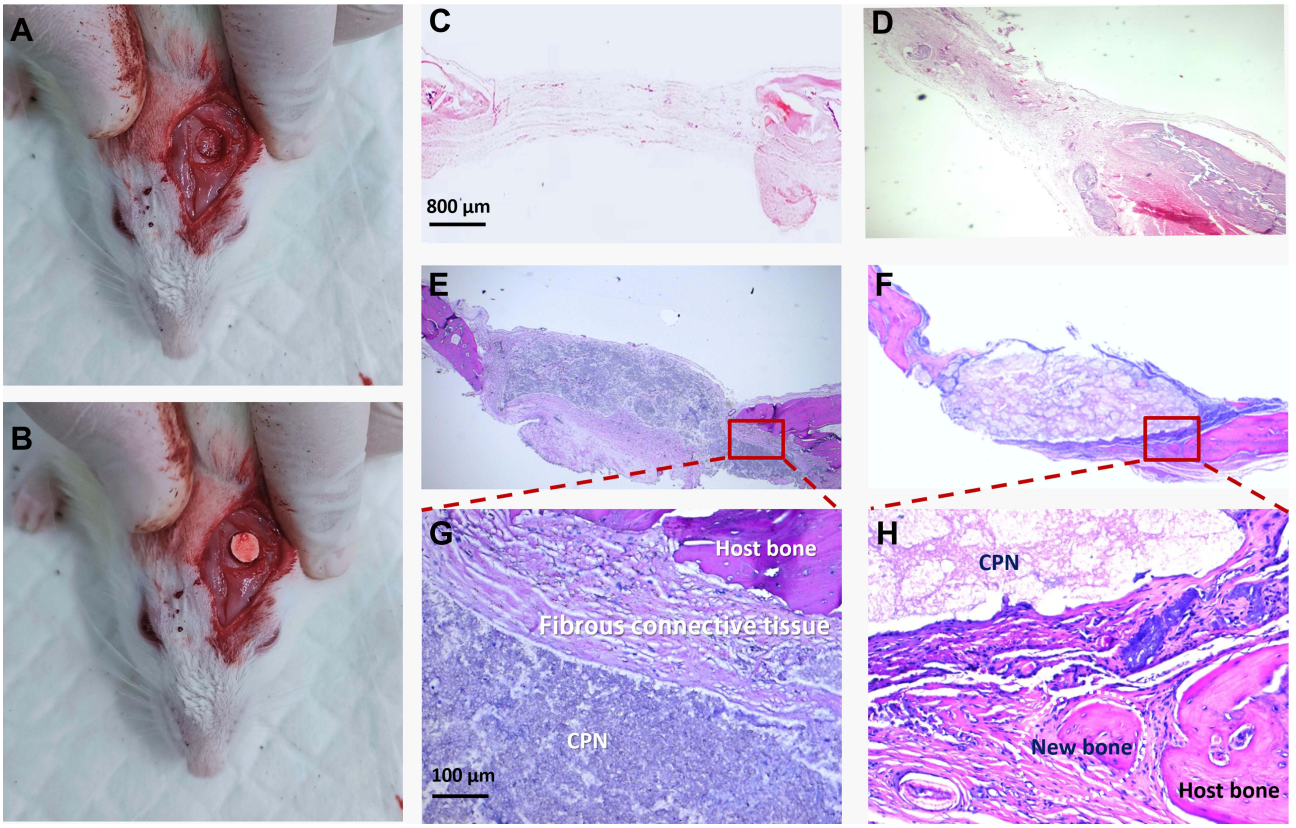

Figure 7 Histological analysis of the calcium phosphate–based nanocomposite (CPN) after implantation in a rat cranial defect model.
Notes: (**A**) A rat critical-size cranial defect model; (**B**) CPN sample (volume = 28.26 mm^3) implantation; (**C**) Blank control at 4 weeks (scale bar=800μm); (**D**) Blank control at 12 weeks (scale bar=800μm); (**E**) The boundary of CPN was smooth after 4 weeks (scale bar=800μm); (**F**) The CPN partly degraded and bone ingrowth was observed at 12 weeks (scale bar=800μm). (**G**) The high-magnification image of E (scale bar=100μm); (**H**) The high-magnification image of F (scale bar=100μm); The red boxes show the condition of osseointegration and CPN biodegradation on the bone-cement interface.
Abbreviation: CPN, calcium phosphate–based nanocomposite.

development of not only robust but also bioactive and absorbable augmentation materials. To overcome some of the shortcomings of PMMA, some studies have focused on the modification of PMMA. Phakatkar et al[41] proposed two-dimensional magnesium phosphate nanosheets and hydroxyapatite nanofibers as novel fillers in PMMA bone cement nanocomposites. They found that the novel nanocomposite significantly enhanced the compressive strength and showed excellent bioactivity and cytocompatibility. Aghyarian et al[31] designed a new composite bone cement developed by introducing hydroxyapatite and brushite to an acrylic two-solution cement at varying concentrations. This kind of cement exhibited increased viscosity, good injectability, and similar gel point time compared with the all-acrylic cement. The cement showed an average compressive strength of 85 MPa, which was slightly lower than that of PMMA measured in our study. For screw augmentation, however, this kind of modified PMMA tends to exhibit excessive mechanical strength or stiffness and does not offer satisfying biodegradation and osseointegration, which are derived from its intrinsic material properties and are difficult to change. Calcium phosphate used to be considered a potential alternative to PMMA, because of its advantages, such as high biodegradability and similarity to host bone.[19,32] It also has shortcomings, however, such as low mechanical strength or robustness, and fast biodegradation when it comes to the purpose of pedicle screw augmentation.[32,33] Hence, modified materials based on calcium phosphate are promising. Aghyarian et al[31] found that a calcium phosphate introduction into their new material improved the properties of viscosity, pseudoplasticity, mechanical strength, and osseointegration. Roozbahani et al[25] developed an injectable nano-calcium phosphate cement and found that the nanostructure could improve mechanical properties, degradation rate, and osteoinduction. No studies, however, have focused on CBT screw augmentation using these mentioned materials.

The current construction of the CPN is a good alternative to PMMA for CBT screw augmentation. First of all, previous studies have shown that the gelatinized starch nanonetwork could greatly improve the injectability of CPC.[26–28,42] A previous in vitro study confirmed its merit of injectability in that the CPN revealed a more consistent injection force pattern than PMMA did.[42] The initial setting time of the CPN was similar to that of PMMA, while the final setting time was slightly shorter than that of PMMA, which was favorable for the intraoperative manipulation of cement augmentation. The peak temperature during CPN setting was about 31°C, which was different from the obvious exothermic phenomenon in the PMMA hardening. Additionally, the introduction of nanostarch also significantly increased the compressive strength of CPC, with the average compression strength up to 40.15 MPa, nearly half that of PMMA, which is in agreement with the previously reported result.[27] This value was obviously improved considering that we have found that the compression strength of CPC was only up to 13.21±2.45 MPa.[27] The compressive strength of CPN is also higher than that of the other newly constructed cements. Roozbahani et al[25] found that the compression strength of their nano-calcium phosphate bone cement based on Si-stabilized α-tricalcium phosphate was increased to 18.70 ± 2.23 MPa. Zhang et al[34] showed that their novel injectable magnesium/calcium sulfate hemihydrate composite reached a maximum value of 18.6 ± 2.7 MPa. Hence, the CPN could be appropriate for CBT screw augmentation from a mechanical point of view.

In previous studies on CPN-augmented traditional cannulated pedicle, we found that CPN exhibited a similar biomechanical property to PMMA.[27,28,42] The current biomechanical pattern of the CPN-augmented CBT technique is consistent with that seen with pedicle screw augmentation. We found that the average Fmax of CPN-augmented CBT screws was similar to that of PMMA-augmented ones. The Fmax of PMMA presented a more discrete data while that of CPN was relatively concentrated. Although the average torque value in the CPN group was lower than that in the PMMA group, there was no statistically significant difference. As expected, regardless of whether PMMA or CPN was used, the biomechanical strength of the cemented CBT screws was greater than that of cement-augmented pedicle screws reported in the aforementioned previous studies, illustrating the effectiveness and superiority of the CPN-augmented CBT technique. The advantage of the CBT screws over traditional pedicle screws is in the greater contact made between the proximal portion of the screws and the harder pedicle cortical bone. The distal part of the screws, which is more likely to make contact with the relatively more spongy vertebral bone, might serve as an important location to further enhance screw stability. The CPN showed a better ability to disperse to the distal areas of the screws and was more likely to form a concentrated cloud mass, which might account for the observation that the CPN showed a satisfactory biomechanical performance, although the CPN could not surpass PMMA in terms of basic mechanical properties reflected by the compressive properties.

Another merit of CPN is that it showed a suitable biodegradation speed that matched the new bone formation. Histological analysis revealed that the CPN was degraded but not collapsed after 12 weeks, when it was critical for the bone fusion after surgery.[43] Once the fusion was achieved, the residual injected CPN should be biodegraded and replaced by new bone tissue. We found that the newly formed bone tightly surrounded the residual CPN clot and kept a good bone–cement interface during the biodegradation. The CPN would eventually be degraded for a longer period, and we have found that only a third of the CPN volume remained after 8-month implantation (unpublished data), which could solve the problems brought about by long-time residual PMMA.

Our study also has some limitations. First, because this study was an in vitro cadaveric biomechanical investigation, the CBT screw placement procedure may have had some different operational details in comparison with clinical practice, especially without X-ray or CT navigation. However, the employment of 3D-printed guide plates likely mitigated the difficulty of the CBT technique to some extent and ensured standardized screw placements. Second, the biomechanical test of pullout strength might not have completely reflected the physiological mechanism of screw loosening in vivo; thus, further evidence should be gathered to verify the viability of this combination of techniques of cement augmentation and CBT screw placement. Furthermore, as donated human cadaveric spine resources are precious, the number of specimens used in this biomechanical study was limited. Additionally, the clinical application of the CPN must be further evaluated in practice.

Conclusion

A novel nanocomposite cement with biocompatibility, CPN, could increase the biomechanical strength of CBT screws. Although it is still slightly weaker than the traditional PMMA, being biocompatible and osteoinductive, CPN has a better dispersion pattern and is a valuable alternative to PMMA augmentation.

Acknowledgments

The authors acknowledge the Natural Science Foundation of Beijing Municipality, China (7212117), the National Key Research and Development Program of China (2020YFC1107401), the National Natural Science Foundation of China (82025025), the Expert Workstation of Yunnan Province of China (202205AF150025), and the Innovation Fund of National Clinical Research Center for Orthopedics, Sports Medicine and Rehabilitation of China (2021-NCRC-CXJJ-ZH-17). The authors thank Ziniu Tang and Xiexing Wu (Soochow University, China) for assistance of the animal study.

Disclosure

Professor Lei Yang reports grants from NSFC, China, grants from MOST, China, during the conduct of the study. The authors report no conflicts of interest related to this work.

References

1. Galbusera F, Volkheimer D, Reitmaier S, Berger-Roscher N, Kienle A, Wilke HJ. Pedicle screw loosening: a clinically relevant complication? *Eur Spine J*. 2015;24(5):1005–1016. doi:10.1007/s00586-015-3768-6
2. Delgado-Fernandez J, García-Pallero M, Blasco G, Pulido-Rivas P, Sola RG. Review of cortical bone trajectory: evidence of a new technique. *Asian Spine J*. 2017;11(5):817–831. doi:10.4184/asj.2017.11.5.817
3. Sakaura H, Miwa T, Yamashita T, Kuroda Y, Ohwada T. Posterior lumbar interbody fusion with cortical bone trajectory screw fixation versus posterior lumbar interbody fusion using traditional pedicle screw fixation for degenerative lumbar spondylolisthesis: a comparative study. *J Neurosurg Spine*. 2016;25(5):591–595. doi:10.3171/2016.3.SPINE151525
4. Crawford CH 3rd, Owens RK 2nd, Djurasovic M, Gum JL, Dimar JR 2nd, Carreon LY. Minimally-Invasive midline posterior interbody fusion with cortical bone trajectory screws compares favorably to traditional open transforaminal interbody fusion. *Heliyon*. 2019;5(9):e02423. doi:10.1016/j.heliyon.2019.e02423
5. Wray S, Mimran R, Vadapalli S, Shetye SS, McGilvray KC, Puttlitz CM. Pedicle screw placement in the lumbar spine: effect of trajectory and screw design on acute biomechanical purchase. *J Neurosurg Spine*. 2015;22(5):503–510. doi:10.3171/2014.10.SPINE14205
6. Akpolat YT, Inceoğlu S, Kinne N, Hunt D, Cheng WK. Fatigue performance of cortical bone trajectory screw compared with standard trajectory pedicle screw. *Spine*. 2016;41(6):E335–341. doi:10.1097/BRS.0000000000001233
7. Matsukawa K, Yato Y. Lumbar pedicle screw fixation with cortical bone trajectory: a review from anatomical and biomechanical standpoints. *Spine Surg Relat Res*. 2017;1(4):164–173. doi:10.22603/ssrr.1.2017-0006
8. Liu L, Zhang S, Liu G, Yang B, Wu X. Early clinical outcome of lumbar spinal fixation with cortical bone trajectory pedicle screws in patients with osteoporosis with degenerative disease. *Orthopedics*. 2019;42(5):e465–e471. doi:10.3928/01477447-20190604-01
9. Janssen I, Ryang YM, Gempt J, et al. Risk of cement leakage and pulmonary embolism by bone cement-augmented pedicle screw fixation of the thoracolumbar spine. *Spine J*. 2017;17(6):837–844. doi:10.1016/j.spinee.2017.01.009
10. Ulusoy OL, Kahraman S, Karalok I, et al. Pulmonary cement embolism following cement-augmented fenestrated pedicle screw fixation in adult spinal deformity patients with severe osteoporosis (analysis of 2978 fenestrated screws). *Eur Spine J*. 2018;27(9):2348–2356. doi:10.1007/s00586-018-5593-1
11. Tavakoli M, Bakhtiari SSE, Karbasi S. Incorporation of chitosan/graphene oxide nanocomposite in to the PMMA bone cement: physical, mechanical and biological evaluation. *Int J Biol Macromol*. 2020;149:783–793. doi:10.1016/j.ijbiomac.2020.01.300
12. Li C, Sun J, Shi K, et al. Preparation and evaluation of osteogenic nano-MgO/PMMA bone cement for bone healing in a rat critical size calvarial defect. *J Mater Chem B*. 2020;8(21):4575–4586. doi:10.1039/D0TB00074D
13. Jacobs E, Saralidze K, Roth AK, et al. Synthesis and characterization of a new vertebroplasty cement based on gold-containing PMMA microspheres. *Biomaterials*. 2016;82:60–70. doi:10.1016/j.biomaterials.2015.12.024
14. He X, Qu Y, Peng J, Peng T, Qian Z. A novel botryoidal aramid fiber reinforcement of a PMMA resin for a restorative biomaterial. *Biomater sci*. 2017;5(4):808–816. doi:10.1039/C6BM00939E
15. Hart RA, Marshall LM, Hiratzka SL, Kane MS, Volpi J, Hiratzka JR. Functional limitations due to stiffness as a collateral impact of instrumented arthrodesis of the lumbar spine. *Spine*. 2014;39(24):E1468–1474. doi:10.1097/BRS.0000000000000595
16. Park JW, Park SM, Lee HJ, Lee CK, Chang BS, Kim H. Infection following percutaneous vertebral augmentation with polymethylmethacrylate. *Arch Osteoporos*. 2018;13(1):47. doi:10.1007/s11657-018-0468-y
17. Yi S, Rim DC, Park SW, Murovic JA, Lim J, Park J. Biomechanical comparisons of pull out strengths after pedicle screw augmentation with hydroxyapatite, calcium phosphate, or polymethylmethacrylate in the cadaveric spine. *World Neurosurg*. 2015;83(6):976–981. doi:10.1016/j.wneu.2015.01.056
18. Chow LC, Takagi S. A natural bone cement-a laboratory novelty led to the development of revolutionary new biomaterials. *J Res Natl Inst Stand Technol*. 2001;106(6):1029–1033. doi:10.6028/jres.106.053
19. Ambard AJ, Mueninghoff L. Calcium phosphate cement: review of mechanical and biological properties. *J prosthodontics*. 2006;15(5):321–328. doi:10.1111/j.1532-849X.2006.00129.x
20. Klein R, Tetzlaff R, Weiss C, et al. Osteointegration and resorption of intravertebral and extravertebral calcium phosphate cement. *Clin Spine Surg*. 2017;30(3):E291–e296. doi:10.1097/BSD.0b013e3182aab2df
21. Lu Q, Liu C, Wang D, Liu H, Yang H, Yang L. Biomechanical evaluation of calcium phosphate-based nanocomposite versus polymethylmethacrylate cement for percutaneous kyphoplasty. *Spine j*. 2019;19(11):1871–1884. doi:10.1016/j.spinee.2019.06.007
22. Blattert TR, Jestaedt L, Weckbach A. Suitability of a calcium phosphate cement in osteoporotic vertebral body fracture augmentation: a controlled, randomized, clinical trial of balloon kyphoplasty comparing calcium phosphate versus polymethylmethacrylate. *Spine*. 2009;34(2):108–114. doi:10.1097/BRS.0b013e31818f8bc1

23. Grafe IA, Baier M, Nöldge G, et al. Calcium-phosphate and polymethylmethacrylate cement in long-term outcome after kyphoplasty of painful osteoporotic vertebral fractures. *Spine*. 2008;33(11):1284–1290. doi:10.1097/BRS.0b013e3181714a84
24. No YJ, Roohani-Esfahani SI, Zreiqat H. Nanomaterials: the next step in injectable bone cements. *Nanomedicine*. 2014;9(11):1745–1764. doi:10.2217/nnm.14.109
25. Roozbahani M, Alehosseini M, Kharaziha M, Emadi R. Nano-calcium phosphate bone cement based on Si-stabilized α-tricalcium phosphate with improved mechanical properties. *Mater Sci Eng C Mater Biol Appl*. 2017;81:532–541. doi:10.1016/j.msec.2017.08.016
26. Liu H, Guan Y, Wei D, Gao C, Yang H, Yang L. Reinforcement of injectable calcium phosphate cement by gelatinized starches. *J Biomed Mater Res B Appl Biomater*. 2016;104(3):615–625. doi:10.1002/jbm.b.33434
27. Sun H, Liu C, Liu H, et al. A novel injectable calcium phosphate-based nanocomposite for the augmentation of cannulated pedicle-screw fixation. *Int J Nanomedicine*. 2017;12:3395–3406. doi:10.2147/IJN.S131962
28. Sun H, Liu C, Li X, et al. A novel calcium phosphate-based nanocomposite for the augmentation of cement-injectable cannulated pedicle screws fixation: a cadaver and biomechanical study. *J Orthop Translat*. 2020;20:56–66. doi:10.1016/j.jot.2019.08.001
29. Wang Y, Yang L, Li C, Sun H. A biomechanical study on cortical bone trajectory screw fixation augmented with cement in osteoporotic spines. *Global Spine j*. 2022;21925682211070826. doi:10.1177/21925682211070826
30. Driessens F, Boltong MG, Bermudez O, Planell JA. Formulation and setting times of some calcium orthophosphate cements: a pilot study. *J Mater Sci*. 1993;4(5):503–508.
31. Aghyarian S, Rodriguez LC, Chari J, et al. Characterization of a new composite PMMA-HA/Brushite bone cement for spinal augmentation. *J Biomater Appl*. 2014;29(5):688–698. doi:10.1177/0885328214544770
32. O'Neill R, McCarthy HO, Montufar EB, et al. Critical review: injectability of calcium phosphate pastes and cements. *Acta biomaterialia*. 2017;50:1–19. doi:10.1016/j.actbio.2016.11.019
33. Miño-Fariña N, Muñoz-Guzón F, López-Peña M, et al. Quantitative analysis of the resorption and osteoconduction of a macroporous calcium phosphate bone cement for the repair of a critical size defect in the femoral condyle. *Vet j*. 2009;179(2):264–272. doi:10.1016/j.tvjl.2007.09.011
34. Zhang S, Yang K, Cui F, et al. A novel injectable magnesium/calcium sulfate hemihydrate composite cement for bone regeneration. *Biomed Res Int*. 2015;2015:297437. doi:10.1155/2015/297437
35. Santoni BG, Hynes RA, McGilvray KC, et al. Cortical bone trajectory for lumbar pedicle screws. *Spine j*. 2009;9(5):366–373. doi:10.1016/j.spinee.2008.07.008
36. Baluch DA, Patel AA, Lullo B, et al. Effect of physiological loads on cortical and traditional pedicle screw fixation. *Spine*. 2014;39(22):E1297–1302. doi:10.1097/BRS.0000000000000553
37. Matsukawa K, Yato Y, Kato T, Imabayashi H, Asazuma T, Nemoto K. In vivo analysis of insertional torque during pedicle screwing using cortical bone trajectory technique. *Spine*. 2014;39(4):E240–245. doi:10.1097/BRS.0000000000000116
38. Li HM, Zhang RJ, Gao H, et al. Biomechanical fixation properties of the cortical bone trajectory in the osteoporotic lumbar spine. *World Neurosurg*. 2018;119:e717–e727. doi:10.1016/j.wneu.2018.07.253
39. McLachlin SD, Al Saleh K, Gurr KR, Bailey SI, Bailey CS, Dunning CE. Comparative assessment of sacral screw loosening augmented with PMMA versus a calcium triglyceride bone cement. *Spine*. 2011;36(11):E699–704. doi:10.1097/BRS.0b013e3181fb73ea
40. Kiyak G, Balikci T, Heydar AM, Bezer M. Comparison of the pullout strength of different pedicle screw designs and augmentation techniques in an osteoporotic bone model. *Asian Spine J*. 2018;12(1):3–11. doi:10.4184/asj.2018.12.1.3
41. Phakatkar AH, Shirdar MR, Qi ML, et al. Novel PMMA bone cement nanocomposites containing magnesium phosphate nanosheets and hydroxyapatite nanofibers. *Mater Sci Eng C Mater Biol Appl*. 2020;109:110497. doi:10.1016/j.msec.2019.110497
42. Sun H, Liu C, Chen S, et al. Effect of surgical factors on the augmentation of cement-injectable cannulated pedicle screw fixation by a novel calcium phosphate-based nanocomposite. *Front Med*. 2019;13(5):590–601. doi:10.1007/s11684-019-0710-z
43. Formica M, Vallerga D, Zanirato A, et al. Fusion rate and influence of surgery-related factors in lumbar interbody arthrodesis for degenerative spine diseases: a meta-analysis and systematic review. *Musculoskelet Surg*. 2020;104(1):1–15. doi:10.1007/s12306-019-00634-x